SANDIA REPORT
SAND2009-0841
Unlimited Release
Printed February 2009

EEG Analyses with SOBI

Akaysha Tang and Matthew R. Glickman

Prepared by
Sandia National Laboratories
Albuquerque, New Mexico 87185 and Livermore, California 94550

Sandia is a multiprogram laboratory operated by Sandia Corporation,
a Lockheed Martin Company, for the United States Department of Energy's
National Nuclear Security Administration under Contract DE-AC04-94AL85000.

Sandia National Laboratories

Issued by Sandia National Laboratories, operated for the United States Department of Energy by Sandia Corporation.

Available to DOE and DOE contractors from
U.S. Department of Energy
Office of Scientific and Technical Information
P.O. Box 62
Oak Ridge, TN 37831

Telephone: (865) 576-8401
Facsimile: (865) 576-5728
E-Mail: reports@adonis.osti.gov
Online ordering: http://www.osti.gov/bridge

Available to the public from
U.S. Department of Commerce
National Technical Information Service
5285 Port Royal Rd.
Springfield, VA 22161

Telephone: (800) 553-6847
Facsimile: (703) 605-6900
E-Mail: orders@ntis.fedworld.gov
Online order: http://www.ntis.gov/help/ordermethods.asp?loc=7-4-0#online

SAND2009-0841
Unlimited Release
Printed February 2009

EEG ANALYSES WITH SOBI

Akaysha Tang
1 University of New Mexico
Logan Hall
MSC03 2220
Albuquerque, NM 87131-1161

Matthew R. Glickman
Cognitive Systems Research and Applications
Sandia National Laboratories
P.O. Box 5800
Albuquerque, New Mexico 87185-MS1004

Abstract

The motivating vision behind Sandia's MENTOR/PAL[1] LDRD project has been that of systems which use real-time psychophysiological data to support and enhance human performance, both individually and of groups. Relevant and significant psychophysiological data being a necessary prerequisite to such systems, this LDRD has focused on identifying and refining such signals. The project has focused in particular on EEG (electroencephalogram) data as a promising candidate signal because it (potentially) provides a broad window on brain activity with relatively low cost and logistical constraints. We report here on two analyses performed on EEG data collected in this project using the SOBI (Second Order Blind Identification) algorithm to identify two independent sources of brain activity: one in the frontal lobe and one in the occipital. The first study looks at directional influences between the two components, while the second study looks at inferring gender based upon the frontal component.

---

[1] The term MENTOR/PAL refers to a specific system architecture where each individual in a group charged with a cooperative task is supported by one personally dedicated computer (a PAL), and where one additional, central system is concerned with the entire group (their MENTOR).

ACKNOWLEDGMENTS

We warmly thank the many students, post-docs, and other collaborators who have contributed to this research, including Mingzhou Ding, Amy Korzekwa, Masato Nakazawa, Matthew T. Sutherland, Peng Sun, and Zhen Yang.

CONTENTS

FIGURES

TABLES

NOMENCLATURE

BSS	Blind Source Separation
DOE	Department of Energy
EEG	Electroencephalogram
SOBI	Second-Order Blind Identification
SNL	Sandia National Laboratories
SVM	Support Vector Machine

1. DIRECTIONAL INFLUENCES BETWEEN TOP-DOWN AND BOTTOM-UP PROCESSING[2]

1.1. Introduction

1.1.1. SOBI

Second-order blind identification (SOBI) (Belouchrani, Abed-Meraim, Cardoso, & Moulines, 1997) is an emerging signal processing technique that can be used to facilitate source analysis from high-density EEG. Similar to other ICA algorithms that have been applied to EEG data (Bell & Sejnowski, 1995), (Hyvarinen & Oja, 1997), SOBI can be used to isolate and remove ocular artifact (Joyce, Gorodnitsky, & Kutas, 2004). In our laboratory, we have conducted extensive investigations to demonstrate the utility of SOBI in aiding source localization from high-density EEG. Specifically, we have shown that (Belouchrani, Abed-Meraim, Cardoso, & Moulines, 1997) SOBI can correctly recover known noise sources (noisy sensors and artificially injected noise at known electrodes) and known neuronal sources (SI activation by median nerve stimulation) (Tang, Liu, & Sutherland, Recovery of Correlated Neuronal Sources From EEG: The Good and Bad Ways of Using SOBI, 2005), (Bell & Sejnowski, 1995) SOBI can increase signal to noise ratio leading to improved performance in single-trial ERP classification (Tang, Sutherland, & Wang, Contrasting Single-Trial ERPs Between Experimental Manipulations: Improving Differentiability by Blind Source Separation, 2006), (Hyvarinen & Oja, 1997) SOBI can recover neuronal sources whose activation are correlated (Tang, Liu, & Sutherland, Recovery of Correlated Neuronal Sources From EEG: The Good and Bad Ways of Using SOBI, 2005); (Joyce, Gorodnitsky, & Kutas, 2004) SOBI can recover neuronal sources using EEG collected when the brain is in its default mode (“resting” state) (Sutherland & Tang, Blind Source Separation Can Recover Systematically Distributed Neuronal Sources From "Resting" EEG, 2006); (Tang, Sutherland, & McKinney, Validation of SOBI Components From High Density EEG, 2005) SOBI can recover neuronal sources during free viewing of continuous streams of visual information (Tang, et al., Classifying Single-Trial ERPs From Visual and Frontal Cortex During Free Viewing, 2006); finally, SOBI can recover weak neuronal signals that temporally overlay with much stronger signals (e.g. signals associated with ipsilateral activation of primary somatosensory cortex) (Sutherland & Tang, Reliable Detection of Bilateral Activation in Human Primary Somatosensory Cortex by Unilateral Median Nerve Stimulation, 2006).

1.1.2. Chapter Goals

In this chapter, we set out to achieve three goals. First, we seek to provide further validation for SOBI recovered neuronal sources by investigating whether the same neuronal sources can be recovered from repeated EEG measures that are obtained days and weeks apart. Second, we

---

[2] Substantial portions of this chapter have appeared as “Top-Down versus Bottom-up Processing in the Human Brain: Distinct Directional Influences Revealed by Integrating SOBI and Granger Causality”, by Akaysha C. Tang, Matthew T. Sutherland, Peng Sun, Yan Zhang, Masato Nakazawa, Amy Korzekwa, Zhen Yang, and Mingzhou Ding in Advances in Cognitive Neurodynamics ICCN 2007: Proceedings of the International Conference on Cognitive Neurodynamics, copyright Springer Science + Business Media, Dordrecht.

combine SOBI with Granger causality analysis to show distinct patterns of theta/alpha contribution in the feed-forward and feedback influences between the frontal and occipital cortices. Third, we investigate how such asymmetrical influence between the frontal and occipital cortices is modulated by sensory processing and by situational familiarity.

1.2. Methods

Eight right-handed subjects volunteered to participate in the present study. All subjects were free of any history of neurological or psychological disorders. The experimental procedures were conducted in accordance with the Human Research Review Committee at the University of New Mexico. Each subject was tested in three sessions at Week 0, Week 1, and Week 4 or later. Up to 7 min of continuous 128-channel EEG data were collected at 1000 or 2000 Hz during: (Belouchrani, Abed-Meraim, Cardoso, & Moulines, 1997) eyes-closed "resting"; (Bell & Sejnowski, 1995) eyes-open "resting"; (Bell & Sejnowski, 1995) video-viewing (a silently played nature video); (Joyce, Gorodnitsky, & Kutas, 2004) listening to only the audio track of the video; and (Tang, Sutherland, & McKinney, Validation of SOBI Components From High Density EEG, 2005) forming mental images of scenes from the video. This chapter limits the discussion to conditions 1-3.

SOBI was applied to the continuous EEG data **x**(t), across all conditions to extract the continuous time course of activation from two types of neuronal components--- anterior (A) and posterior (P) components. For details on SOBI application, see (Tang, Sutherland, & McKinney, Validation of SOBI Components From High Density EEG, 2005). Briefly, SOBI recovers the underlying sources, **s**(t), by minimizing the sum squared cross-correlations between $\mathbf{s}_i(t)$ and $\mathbf{s}_j(t+\tau)$, across all pairs of sources and across multiple time delays τs. A subset of SOBI-recovered components can be verified as neuronal sources via source localization using a forward model (e.g. BESA 5.0) (Hyvarinen & Oja, 1997). Here we focused our analysis on two such neuronal components that correspond to focal regions within the frontal and occipital lobes.

Feed-forward (FF) and feedback (FB) influences were quantified by Granger causality between the two components, reflecting long-distance *directional* influences between the frontal and occipital cortices. Granger causality analysis was carried out on the continuous time courses, $\mathbf{s_i}(t)$, for the selected components A and P according to methods detailed in (Ding, Short-Window Spectral Analysis of Cortical Even-Related Potentials by Adaptive Multivariate Autoregressive Modeling: Data Preprocessing, Model Validation, and Variability Assessment, 2000), (Ding, Chen, & Bressler, Granger Causality: Basic Theory and Application to Neuroscience, 2006). As Granger causality can be decomposed into its frequency content, we computed Granger causality spectrum and measured power within the theta (4-7 Hz) and alpha (8-14 Hz) bands using a moving window of 30-sec with 5-sec increments. Power of anterior and posterior components in theta and alpha bands were also computed as indicators of synchronization within the local networks.

1.3. Results

*Reliable Extraction and Identification of Neuronal Components from Repeated Measures made Weeks Apart***.** In all 8 subjects, across all 3 sessions, we were able to recover SOBI components that corresponded to two distinct neuronal sources, one localized to a rather focal region within the frontal cortex, in or near anterior cingulate cortex (ACC) and the other to focal regions within the occipital lobe (occipital gyrus). Repeated- measure ANOVA revealed no statistically significant differences in the location of the corresponding ECD models across the 3 recording sessions. As no session-to-session difference was found, the average locations across the 3 sessions are shown in Figure 1.1. ECDs for each of the 8 subjects are superimposed in the figure revealing a tight clustering of ECDs across subjects. This result demonstrates that SOBI can reliably recover components that correspond to anatomically well defined brain regions even when the recording sessions were made weeks apart.

It is important to emphasize that the recovery of these two neuronal sources was achieved without imposing constraints of fixation and use of event-related stimulation paradigms. Instead, the subjects were allowed to freely move or blink their eyes as needed during the recording conditions. No segment of EEG data was excluded prior to the application of SOBI. These unique features of SOBI processing have non-trivial implications for the study of mental disorders and the study of early development or aging where subjects are often unable to conform to typical experimental constraints.

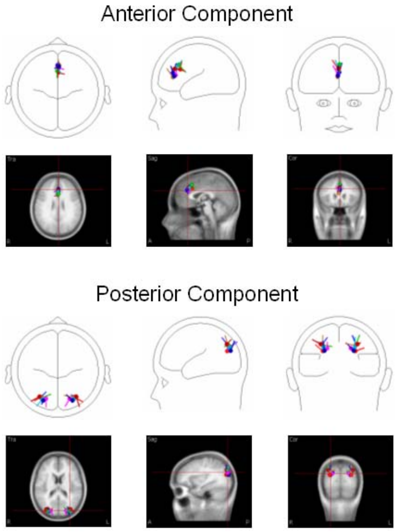

Figure 1.1 Equivalent current dipole (ECD) locations for the SOBI recovered anterior and posterior neuronal components.

Theoretically, this result implies that SOBI's ability to recover anatomically well-defined neuronal sources does not depend upon the use of any event-related stimulation paradigm. Thus, fast brain electrical activity in the default mode (Gusnard & Raichle, 2001) can be investigated in terms of neuronal signals originating from specific focal cortical areas. In comparison to the default mode brain activity revealed by fMRI, the default mode activity revealed with SOBI and EEG will offer a temporal resolution of millisecond, allowing the characterization of default mode brain dynamics within a new temporal domain.

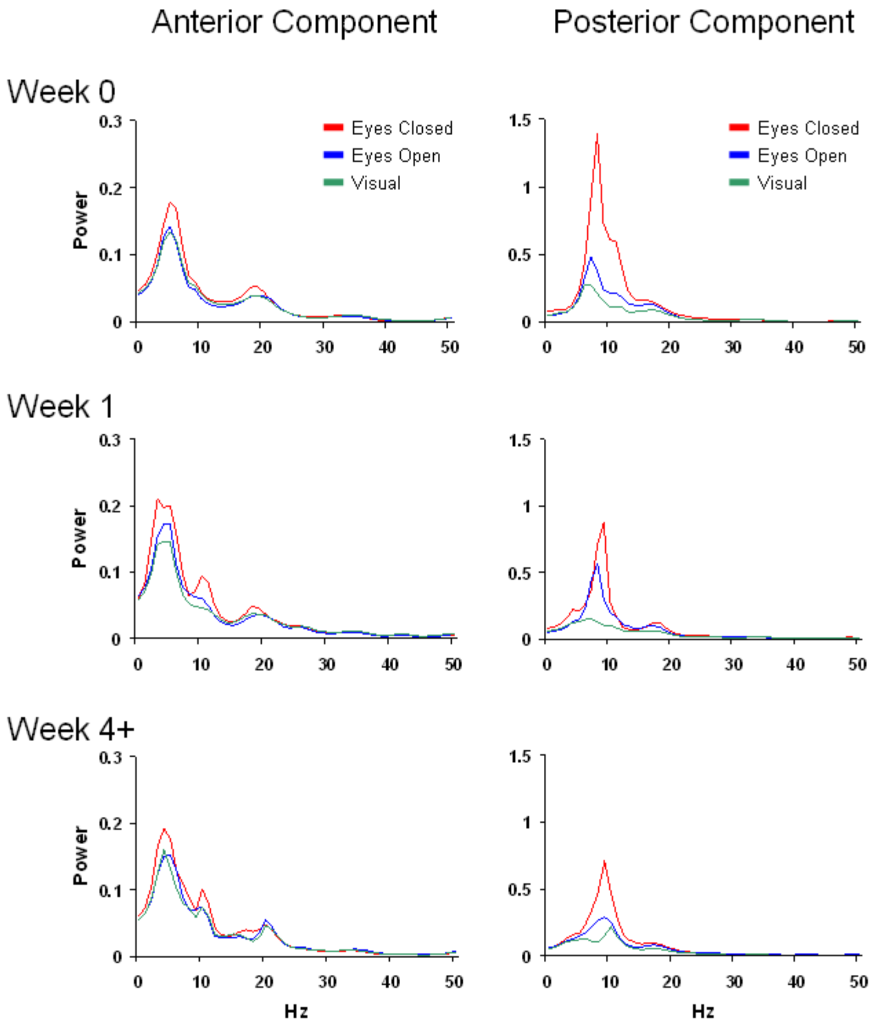

Figure 1.2 Median power spectra of two SOBI-neuronal components as a function of repeated exposures to the same experimental situation. Session 1: week 0; Session 2: week 1; Session 3: week 4+.

Local Network Synchrony Shows Distinct Patterns of Change across 3 Repeated Exposures to the same Experimental Situation. For each of the 3 recording sessions, power spectra from the component time course were computed for ~5-min segments during which the subjects had their eyes-closed (red), eyes-open (blue), or viewed a nature video (green), respectively Figure 1.2.

The anterior component had peak power within the theta band while the posterior component had peak power within the alpha band, indicated by a significant main effect of Region on the theta-to-alpha ratio ($F(1,7) = 52.12$, $p<0.001$, partial eta^2 = 0.88). This is consistent with the well established fact that the posterior and anteiro parts of the brain are major sources of alpha and theta generators respectively.

Power spectra in these two components were differentially modulated by sessions and experimental conditions [interaction effect: Region x Session (contrast coefficients: 1, -1, 0) x Condition (1, 0, 1), $F(1,7) = 3.52$, $p = 0.05$, 1-tailed, partial eta^2=0.33)]. For the posterior component, the power spectra revealed a systematic effect of session and experimental condition. Across the 3 repeated exposures to the same experimental conditions, peak alpha power decreased as the testing situation became increasingly familiar.

Across the 3 experimental conditions, the highest peak alpha power was associated with the eyes closed condition and the alpha peak power was successively reduced when the demand for visual processing increased from the eyes-closed to the eyes-open and video-viewing conditions. This latter observation is consistent with the known observation that visual processing suppresses alpha band activity. In contrast, for the anterior component, the power spectra showed a relative insensitivity to repeated exposures to the same experimental conditions and little modulation by the eyes-closed, eyes-open, and video-viewing conditions.

Differential Modulation of Theta/Alpha Contribution to Feed-Forward and Feedback Influences by Situational Familiarity and Visual Processing FF(posterior-to-anterior) and FB (anterior-to-posterior) influences were measured by Granger causality in the theta and alpha band activity separately. FF and FB Granger causality measures were plotted as a function of time Figure 1.3. For the FF influence, when the eyes were closed, alpha band activity clearly dominates as indicated by the alpha waveforms (black) having greater area underneath the curve than the theta waveforms (grey). This alpha dominance was clearly reduced when the eyes were open and was further reduced to nearly non-existence when the subjects viewed a video. For the FB influence, the pattern of alpha dominance over theta was reversed showing uniform theta dominance over alpha across all 3 experimental conditions.

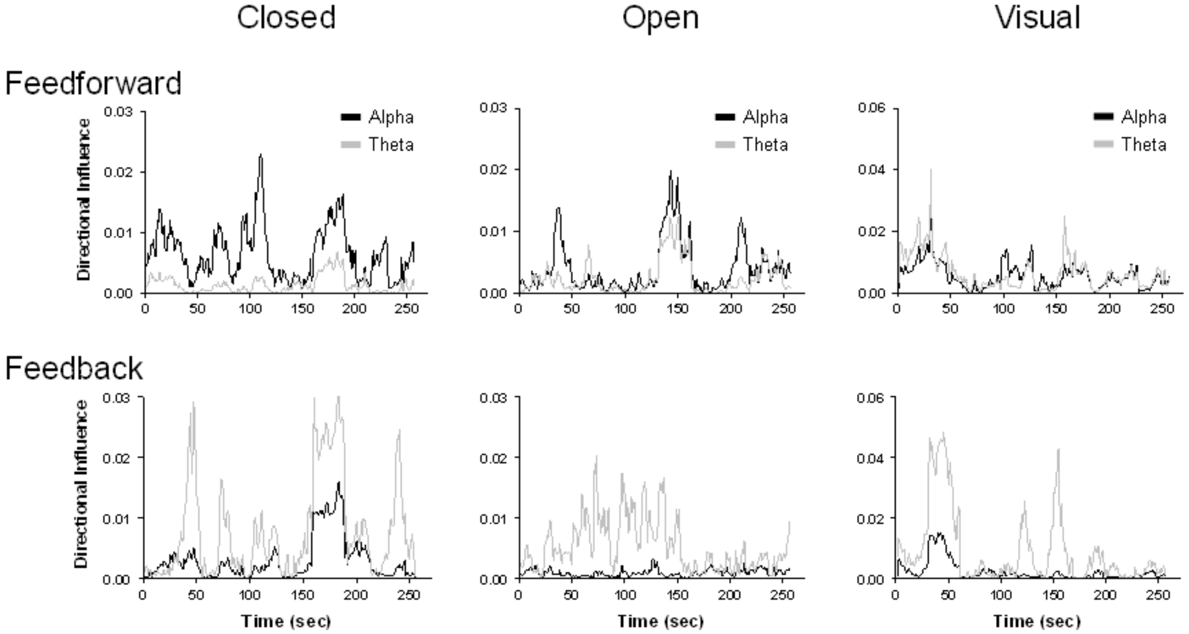

Figure 1.3 Theta dominance over alpha in the anterior-to-posterior feedback influence and its reversal in the posterior-to-anterior feed-forward influence (shown for a single-subject).

Using the area underneath the curve as a dependent measure, we summarize results from all 8 subjects across all three recording sessions in Figure 1.4. To determine whether theta and alpha band activity contribute differentially to the FF and FB influences and how such differential contribution is modulated by situational familiarity and sensory processing, we performed an ANOVA on the theta/alpha ratio.

Theta/alpha ratio differed significantly between the FF and FB influences with a greater ratio for FB influence than for the FF influence (main effect of Direction, $F(1,7) = 34.64$, $p<0.001$, partial

$eta^2 = 0.83$), i.e. a theta dominance in FB influence. This can be seen by the higher measures for the theta band activity than the alpha band activity for the FB influences in most of the 9 conditions and clear reversal or reduction of this theta dominance in the FF influence Figure 1.4.

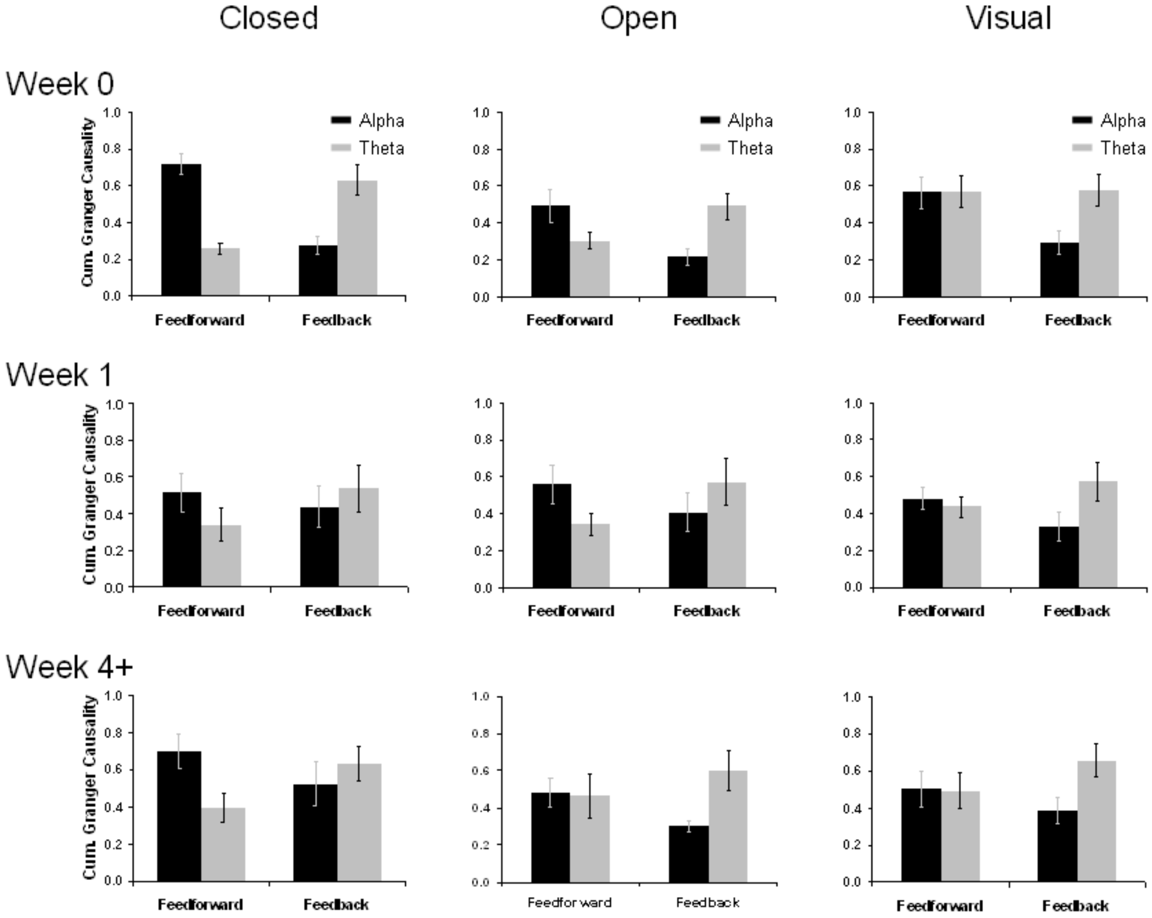

Figure 1.4 Cumulative Granger Causality (area underneath the curve in Figure 1.3) in the theta and alpha band as a function of situational familiarity (repeated sessions) and a function of visual processing (eyes-closed, eyes-open, video-viewing).

This reversal of theta dominance from FF and FB influences was significantly modulated by the familiarity of the situation [Direction x Session (contrast coefficients: 1, -1, 0), $F(1,7) = 11.97$, $p = 0.005$, 1-tailed, partial $eta^2=0.63$]. The reversal is more prominent when the situation was novel (Week 0) than n became more familiar (Week 1 and 4+). This is best seen in the case of eyes-closed condition. The magnitude of reversal is clearly reduced from Week 0 to Week 4+.

For the eyes-open condition, the theta dominance was reversed in Week 0 and 1 and reduced in Week 4+. For the video-viewing condition, the reversal of theta dominance does not appear to be influenced by the increasing situational familiarity. These patterns indicate that the FF / FB contrast is dependent upon the amount of visual information processing involved. When the subjects were engaged in visual perception during the viewing of the video, theta dominance in the FB influence and theta-alpha balance in the feed-forward influence are maintained across recording sessions. This visual processing-dependent effect is supported by a significant 3-way interaction (Direction x Session (1, -1, 0) x Condition (1, 0, -1), $F(1,7) = 7.13$, $p = 0.02$, 1-tailed partial $eta^2=0.63$).

Within Week0 when the recording situation was novel (which is comparable to most studies that do not deal with the issue of task familiarity), theta dominance in the FB influence was maintained despite varying demand for visual processing. In contrast, the alpha dominance in the FF influence in the case of eyes-closed condition was reduced by increasing demand for sensory processing. In fact, visual processing was accompanied not only by a reduction in alpha but an increase in theta band activity in the FF influence. We speculate that this increase in theta band activity serves to "match" the theta-dominance in the FB influence to mediate the dynamic two-way communication between the posterior and anterior parts of the brain.

1.4. Discussion

We analyzed high-density EEG data collected from 8 subjects in three sessions of recording that were weeks apart, each including a period of resting with eyes-closed, resting with eyes-open, and visual perception while free viewing a nature video. We extracted neuronal signals from focal brain regions within the frontal and occipital lobes and showed that such extraction can be achieved under free viewing conditions and from recordings made weeks apart. As many intervening events must have taken place during the intersession intervals, the reliable extraction of the same neuronal sources raises the possibility that such a wide range of variations may be overcome by the use of SOBI in longitudinal experimental designs necessary for developmental and aging studies.

Applying Granger causality analysis to the time courses of the frontal and occipital SOBI components, we presented evidence indicating distinct patterns of theta/alpha band activity in the FF and FB influences between the two components, with a theta dominance characterizing the FB influence and an alpha dominance in the FF influence. By comparing the feed-forward and feedback influences under varying degrees of situational familiarity (sessions) and under conditions of varying degrees of visual processing (eyes-closed, eyes-open, and video viewing), we presented evidence that the balance in theta-alpha band activity between the FF and FB influences is modulated by two factors. First, situational familiarity can reduce the degrees of theta and alpha dominance in the FB and FF influences respectively (as in the case of eyes-closed). Second, the amount of sensory processing increases the theta band contribution and decreases alpha band contribution to FF influence but has little effect on FB influence. Finally, situational familiarity and sensory processing jointly determine the theta-alpha balance. Increasing familiarity and increasing visual processing both *increases* theta band contribution to *FF* influence. In contrast, for *FB* influences, increasing familiarity *decreases* theta band contribution when there is little demand for visual processing (Eyes-closed) and has no effect on theta band contribution when there is high demand for visual processing (Visual).

Together, these findings demonstrate a novel non-invasive approach to the assessment of top-down and bottom-up influences in the human brain. These findings may particularly benefit those clinicians and researchers who are interested in how bottom-up and top-down influences interact in both diseased and normal brains. Future work will extend this analysis to networks involving more functionally distinct brain regions.

2. DETERMINING GENDER FROM LOCAL NETWORK SYNCHRONIZATION IN THE FRONTAL CORTEX[3]

2.1. Introduction

In this chapter, we report results from attempting to distinguish between male and female subjects based solely upon data from the frontal cortex neuronal component introduced in the previous chapter. Using a Support Vector Machine (SVM) for classification, we measured powers in four distinctive frequency bands from many 10 sec time windows of the time series of the frontal cortex signals and used these power values as feature dimensions of inputs to the SVM. With data from all four bands, classification accuracy was found to be above 90%.

This problem is interesting because it may shed light on how the dynamics of ongoing brain activity independent from any goal or task differ between the male and female brains. Such differences in the local ongoing network dynamics may reveal gender differences at a more fundamental level of neural processing than could be revealed under specific task conditions.

2.2. Methods and Results

Support Vector Machines (SVM). SVM is a powerful methodology for solving problems in nonlinear classification, function estimation and density estimation, which has also led to many other recent developments in kernel based methods in general. On many practical problems, SVM has shown superior performance over other classification algorithms, including multilayer neural networks (Muller, Krauledat, Dornhege, Curio, & Blankertz, 2004).

Originally, SVM was introduced within the context of statistical learning theory and structural risk minimization. It guarantees the generalization ability by finding the maximum margin separating hyper-plane; in addition, the solution is given by convex optimization, typically quadratic programming, therefore there is a global optima, not like the multilayer neural networks suffering local minima problem. We consider data points of the form:

$$\{(x_1,c_1),(x_2,c_2),\ldots,(x_n,c_n)\}, x_i \in \Re^N, c_i \in (-1,1),$$

where the c_i is either 1 or −1, a constant denoting the class to which the point x_i belongs. Each x_i is a p-dimensional vector. We denote the separating hyper-plane by W. Least Squares Support Vector Machines (LS-SVM) finds the optimal separating hyper-plane by solving the following minimization problem:

---

[3] Substantial portions of this chapter have appeared as “Determining Gender from Local Network Synchronization in the Frontal Cortex” by P. Sun, Z. Yang, A. Korzekwa, M. T. Sutherland, and A. C. Tang in Proceedings of the 7th International Conference on Independent Component Analysis and Signal Separation (ICA 2007), copyright Springer-Verlag GmbH Berlin Heidelberg.

$$\text{Minimize } \left(\frac{1}{2}\right)\|W\|^2 + \frac{\zeta}{2}\sum_i e_i^{\ 2},$$

$$\text{Subject to } c_i(W \cdot \phi(x_i) - b) = 1 - e_i, \text{ for } 1 \le i \le n,$$

where we introduce slack variables, e_i, which measure the degree of misclassification of the datum x_i; ϕ is a nonlinear mapping function that transform original feature space to higher dimensional space. A very common kernel is Radial Basis Function: $K(x, y) = \exp\left\{-\|x - y\|^2 / 2\sigma^2\right\}$. The mapping function ϕ is given by Mercer's condition, that is $K(x, y) = \phi(x)\phi(y)$.

Data. We apply this LS-SVM to the problem of classifying gender based on a very short segment of brain electrical signal originating from the frontal cortex. For SOBI-aided extraction of frontal neuronal signals from high density EEG and the localization of the frontal signal source, (Tang, et al.), (Tang, Sutherland, & McKinney, Validation of SOBI Components From High Density EEG, 2005).The time series of each of 16 subjects' (8 males and 8 females) identified frontal source is truncated into short overlapping windows (10 sec window with 8 sec overlap); for each window, the power level for each of the following four frequency bands is calculated: theta 3-7Hz, alpha 8-12Hz, beta 13-20Hz, and gamma 21-35Hz. These four quantities set up the feature space for the classification problem; each time window produces a 4-dimensional vector to feed into the SVM.

Training and testing. We adopted the Radial Basis Function (RBF) as the kernel of the SVM, which is nonlinear and mapping the original 4-dimensional feature space to infinite dimensional space. During the training phase of the SVM, 10% of the data from each of the subjects was randomly selected to make up the training set and the remaining 90% as the testing data set. This process is repeated either 50 (Exp 1) or 100 times (Exp 2) in different experiments and average and standard error of means of the accuracy over these repeated sampling will be reported in the table. A two-fold cross-validation method was used to search for the optimal regularization parameters, ζ and σ. A grid search was first performed over a range of the parameter values using half of the training set to find the optimal separating hyper-plane, and the other half to evaluate the performance of the hyper-plane in classification. The final values of the parameters are set as the ones that yielded the best classification accuracy o the training set.

Table 2.1 Classification accuracy using data collected while the subject is resting with eyes closed or engaged in more active.

Condition	**Active Processing**	**Resting (eyes-closed)**
Accuracy	87% +/- 3%	92% +/- 3%

Classification experiment one. To determine whether neuronal signals from more active mental states can help improve gender classification based on signals from passive resting state, we compared classification accuracy using 5 minutes of EEG data collected while the subject was at rest with eyes closed with the accuracy of classification using additional data collected when the subject is at rest with eyes open, is viewing a nature video, and forming mental images of the video. Table 2.1 shows that with only 5 minutes of signal from a resting state, an accuracy of 92% can be achieved. Surprisingly, with 4 times of that data lengths and additional information from more active processing states, accuracy was not improved. We suspect that this decrease may have to do with increased commonality during active processing.

Classification experiment two. To determine whether neuronal signals in a specific frequency band are particularly useful for gender classification, we compared classification accuracy across all sub-spaces of the 4-dimensional feature space. This experiment was performed using only data from eye-closed resting condition. Table 2.2 shows when single band power was used as input, i.e. a single feature was used to represent each 10 sec window, classification accuracy ranged between 63%--73%, with the highest accuracy resulting from Gamma band power as the sole feature. Table 2.3 shows that when combinations of 2 band power were used, classification accuracy increased to 69%--88%. Interestingly, the highest accuracy was reached by gamma-theta and gamma-alpha combinations. Finally, using a 3 band combination, classification accuracy further increased to 86%--91%. Once again, the higher accuracy values involved power in the gamma band as one of the feature dimensions.

Table 2.2 Classification accuracy (%) as function of single frequency band.

Band	θ	α	β	γ
Accuracy	63+/-0.4	66+/-0.6	69+/-0.9	73+/-0.5

Table 2.3 Classification accuracy (%) as a function of 2 band combination.

Band	θ, α	θ, β	θ, γ	α, β	α, γ	β, γ
Accuracy	69+/-0.8	81+/-0.6	88+/-0.6	84+/-0.6	87+/-0.5	78+/-0.9

Table 2.4 Classification accuracy (%) as a function of 3 band combination.

Band	θ, α, β	θ, α, γ	θ, β, γ	α, β, γ
Accuracy	86+/-0.6	89+/-0.4	90+/-0.6	91+/-0.5

2.3. Summary

We showed that using 10% of 5 minutes of SOBI pro-processed data as training set and using only the powers of theta, alpha, beta, and gamma band as input dimensions to the SVM classifier, short 10 sec of waves of electrical signals from the frontal cortex can be classified according the gender of the brain with an accuracy greater than 90%. We found that using more EEG data collected during active cognitive processing did not lead to improvement in classification accuracy and that the gamma band power appeared to be the most important feature in classifying male and female brain signals.

3. REFERENCES

Bell, A. J., & Sejnowski, T. J. (1995). An Information-Maximization Approach to Blind Separation and Blind Deconvolution. *Neural Computation* , 1129-1159.

Belouchrani, A., Abed-Meraim, K., Cardoso, J. F., & Moulines, E. (1997). A Blind Source Separation Technique Using Second-Order Statistics. *IEEE Trans. Signal Process* , 434-444.

Ding, M. (2000). Short-Window Spectral Analysis of Cortical Even-Related Potentials by Adaptive Multivariate Autoregressive Modeling: Data Preprocessing, Model Validation, and Variability Assessment. *Biological Cybernetics* , 35-45.

Ding, M., Chen, Y., & Bressler, S. L. (2006). *Granger Causality: Basic Theory and Application to Neuroscience.* Wiley.

Gusnard, D. A., & Raichle, M. E. (2001). Searching for a Baseline: Functional Imaging and the Resting Human Brain. *Nature Review Neuroscience* , 685-694.

Hyvarinen, A., & Oja, E. (1997). A Fast Fixed-Point Algoithm for Independent Component Analysis. *Neural Computation* , 1483-1492.

Joyce, C. A., Gorodnitsky, I. F., & Kutas, M. (2004). Automatic Removal of Eye Movement and Blink Artifacts from EEG Data Using Blind Component Separation. *Psychopysiology* , 313-325.

Muller, K. R., Krauledat, M., Dornhege, G., Curio, G., & Blankertz, B. (2004). Machine Learning Techniques for Brain-Computer Interfaces. *Biomedical Engineering (Biomedizinische Technik) , 49* (1), 11-22.

Schroder, M., Bogdan, M., Rosenstiel, W., Hinterberger, T., & Birbaumer, N. (2003). Automated EEG Feature Selection for Brain Computr Interfaces. *1st International IEEE EMBS Conference on Neural Engineering.* Capri Island, Italy.

Sutherland, M. T., & Tang, A. C. (2006). Blind Source Separation Can Recover Systematically Distributed Neuronal Sources From "Resting" EEG. *Eurasip Proceedings of the Second International Symposium on Communications, Control, and Signal Processing.* Marrakech, Morocco.

Sutherland, M. T., & Tang, A. C. (2006). Reliable Detection of Bilateral Activation in Human Primary Somatosensory Cortex by Unilateral Median Nerve Stimulation. *NeuroImage* , 1042-1054.

Tang, A. C., Liu, J. Y., & Sutherland, M. T. (2005). Recovery of Correlated Neuronal Sources From EEG: The Good and Bad Ways of Using SOBI. *NeuroImage* , 507-519.

Tang, A. C., Sutherland, M. T., & McKinney, C. J. (2005). Validation of SOBI Components From High Density EEG. *NeuroImage* , 539-553.

Tang, A. C., Sutherland, M. T., & Wang, Y. (2006). Contrasting Single-Trial ERPs Between Experimental Manipulations: Improving Differentiability by Blind Source Separation. *NeuroImage* , 335-346.

Tang, A. C., Sutherland, M. T., McKinney, C. J., Liu, J. Y., Wang, Y., Parra, L. C., et al. (2006). Classifying Single-Trial ERPs From Visual and Frontal Cortex During Free Viewing. *IEEE Proceedings of the International Joint Conference on Neural Networks*, (pp. 1376-1383). Vancouver, BC, Canada.

Tang, A. C., Sutherland, M. T., Sun, P., Yang, Z., Nakazawa, M., Korzekwa, A., et al. Top-down Versus Bottom-up Processing in the Human Brain: Distinct Directional Influences Revealed by Integrating SOBI and Granger Causality. (2007) *7th International Conference on Independent Component Analysis and Signal Separation.*

Vapnik, V. (1998). *Statistical Learning Theory*. New York: Wiley.

DISTRIBUTION

1	MS0123	D. Chavez, LDRD Office	1011
1	MS0899	Technical Library	9536

Sandia National Laboratories